18.

Elasto-plastic behaviour and load-capacity of multi-layered plated structures

18.1. Introduction

This chapter is a review of research realized in last decade mainly in collaboration with the late Professor Katarzyna Kowal-Michalska in the domain of elasto-plastic behaviour and ultimate strength of multi-layered plated structures. Thin plates consisting of several layers are widely used in modern thin-walled structure design. The layers are made of different materials. This concept is connected with common effort to reduce the weight of a structure while maintaining its strength properties. Since the mid-1980s, composite materials have been widely used in numerous engineering applications, also as materials of thin-walled beams and columns. Among them there are fiber composites, fiber metal laminates (FML), functionally graded materials (FGM). A separate class of multi-layered plated structures are sandwich plates: three-layered plates with different types of structural cores (honey comb, corrugated sheets, reinforced foam).

The fibrous composite material consists mostly of two components: the matrix and reinforcement i.e. fibres. The typical modern fibrous composite material is that belonging to the HCTL class (Hybrid Titanium Composite Laminate) and it consists of several layers of titanium and carbon fibres laid alternately [18.26].

Fibrous composites are non-homogenous and anisotropic materials. In particular cases, if fibres are orientated in the matrix in one or two perpendicular directions the composite is the orthotropic material with certain principal directions of orthotropy. If the reinforcement is distributed randomly in the matrix the composite material is isotropic one.

Fiber Metal Laminates (FMLs) are hybrid materials, built from thin layers of metal alloy and fiber reinforced epoxy resin. These materials are manufactured by bonding composite plies to metal ones. FMLs, with respect to metal layers, can be divided into FMLs based on aluminum alloys (ARALL reinforced with aramid fibers, GLARE - glass fibers, CARALL - carbon fibers) and others. Nowadays material such as GLARE (carbon fiber/aluminum) due to their very good fatigue and strength characteristics combined with the low density find

increasing use in aircraft industry. The most common type of aluminium applied in Glare is 2024-T3 Alloy.

The safe work of thin-walled structures subjected to in-plane loading is often determined by local buckling. The methods allowing for estimation of ultimate strength of thin-walled plated structures can be classified into four categories:

- analytical-numerical methods where the equations describing the elastic post-buckling behaviour are found out analytically and next the elasto-plastic state is dealt with on the basis of the theory of plasticity by means of an iterative procedure [18.10],
- the effective width approach, which consists in reduction of the flexural stiffness of the cross-section after local buckling and subsequently - in the implementation of the first yield threshold criterion in order to estimate a load-carrying capacity of the structure (lower bound estimation) [18.10, 18.22],
- numerical methods - finite element methods and finite strip methods are both included in this category [18.25, 18.15],
- kinematical methods based on principle of virtual velocities, leading to the upper-bound estimation of ultimate load [18.13].

18.2. Problem formulation

The aim of the study is the estimation of the ultimate load for rectangular three-layered plates subjected to compression. The load carrying capacity of three-layered plated structures is determined by means of four methods mentioned above. The considered plate elements are simply supported and initially flat. The complex structure is assumed to be built of three-layered plates with metallic isotropic face layers and metallic or composite (orthotropic) core. The following core materials are taken into consideration:

a) metallic,
b) fibrous composite,
c) FML material,
d) honeycomb core.

The loading is applied in such a way that during analysis the response of the plate to the increment of its nodal displacements (Fig. 18.1) is searched for.

The plates are initially flat and stress free. It is assumed that the plate edges are simply supported and remain straight during loading. The plates are built of two identical isotropic layers (faces) that cover the middle layer (a core) of different material than faces.

The plates under consideration can be treated as individual elements (walls) of plated structures such as columns or beams (girders). Determining an ultimate strength of separate plate member allows one to estimate (approximately as a lower bound) the ultimate load of a whole structure.

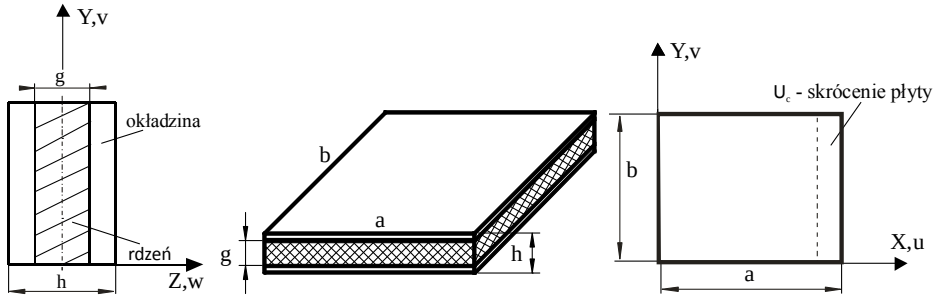

Fig. 18.1. Geometry of the plate

18.3. Review of applied methods of analysis

18.3.1. Analytical-numerical method

The method described below allows one to conduct the analysis of strains and stresses in the elastic and elasto-plastic range and to find out a load-displacement curve for the multi-layered plate. The analysis is carried out on the basis of nonlinear theory of thin plates involving plasticity [18.6, 18.8]. When mechanical properties of all layers are of the same range, the Kirchhoff's hypothesis can be applied for the entire section.

The elastic material properties are determined by following independent constants:

- for outer layers: E_m, ν_m,
- for middle layer (it can be orthotropic in such a way that there are only differences in strengths/yield limits due to positive and negative stresses) - E_c, ν_c,
- the pre-buckling displacement and stress fields of a plate are described by its nodal displacements in the *x* and *y* direction

$$u^o = U_c \frac{x}{a} \tag{18.1}$$

and additionally: $\sigma_x^o = const.$, $\sigma_y^o = 0$, $\tau_{xy}^o = 0$.

In the elastic range the solution of buckling problem and post-buckling behaviour has been obtained on the ground of the classical theory of thin laminated plates [18.10].

In order to obtain the approximate solution of the problem the expressions describing the forms of displacement fields in the elastic range have been found out (the detailed description of the method is given in Refs. [18.6, 18.7]).

The deflection function "*w*" has been assumed as

$$w = f \sin\frac{\pi x}{a}\sin\frac{\pi y}{b} \tag{18.2}$$

where f denotes the free parameter.

Assuming the in-plane displacements u and v in following forms

$$u = u^o + f^2\left(C_1 \sin\frac{2\pi x}{a} + B_1 \sin\frac{2\pi x}{a}\cos\frac{2\pi y}{b}\right) \tag{18.3}$$

$$v = v^o + f^2\left(C_2 \sin\frac{2\pi y}{b} + B_2 \sin\frac{2\pi y}{b}\cos\frac{2\pi x}{a}\right) \tag{18.4}$$

where C_1, C_2, B_1, B_2 are constants depending on the material and geometrical properties of layers that can be found out from equilibrium equations and taking into account boundary conditions. The displacement fields are determined for whole plate in the elastic range.

If the displacements "*u*", "*v*", "*w*" are known then using the von Karman's geometrical relations between strains and displacements and Hooke's law for orthotropic and/or isotropic material the elastic stresses can be determined in any point of a three layered plate.

In aim to determine the ultimate load the analysis of the post-buckling state has to be carried out in the elasto-plastic range. In the plastic range the following assumptions are made:

- the material properties of layers are known in the whole range of stresses,
- the appropriate yield criterion is applied for considered materials,
- all assumptions of non-linear plate theory still hold,
- the forms of displacement functions are the same in the elastic and elasto-plastic range but their amplitude "*f*" can vary arbitrarily,
- according to the plastic flow theory the increments of plastic strains are described by Prandtl-Reuss equations.

Additionally it has been assumed that the material characteristics of isotropic and orthotropic layers are elastic-perfectly plastic. Therefore the following material properties in plastic range are to be applied:

- for isotropic material (faces, core) - σ_{Ym}, σ_{Yc} - yield limit,
- for orthotropic material (a core) - T, C - yield limit in tensile and compression tests in *x* and *y* direction, respectively; and additionally S - yield stress in pure shear.

For orthotropic materials Tsai and Wu proposed the yield (failure) criterion that takes into account the difference in strengths due to positive and negative stresses. In case of a plane stress state Tsai-Wu criterion is formulated as follows

$$F = k_1\sigma_x + k_2\sigma_y + k_3\tau_{xy} + k_{11}\sigma_x^2 + k_{22}\sigma_y^2 - k_{12}\sigma_x\sigma_y + 3k_{33}\tau_{xy}^2 = 1 \tag{18.5}$$

where parameters k_1, k_2, k_3 and $k_{11}, k_{22}, k_{12}, k_{33}$ have to be determined by tensile, compressive and shear tests [18.10].

It is easy to notice that both Hill's yield criterion and Huber-Mises criterion can be obtained from the equation (18.5).

The associated flow rule for a given yield criterion can be expressed as [18.10]

$$d\varepsilon_{ij}^p = \Lambda S_{ij}; \qquad i, j = 1,2,3 \tag{18.6}$$

where: $S_{ij} = \dfrac{1}{3}\dfrac{\partial F}{\partial \sigma_{ij}}; \qquad i, j = 1,2,3.$

The relations (18.6) were formulated by Prandtl and Reuss [18.10].

In the calculations of elasto-plastic plates undergoing large deformations the infinitesimal increments in (18.6) have to be replaced by finite ones (denoted by Δ). Then the relations between stress and strain increments in the elasto-plastic range are described by Prandtl-Reuss equations in a form

$$\begin{aligned}
\Delta\sigma_{\mathrm{x}} &= \frac{E}{(1-\nu^2)}[\Delta\varepsilon_{\mathrm{x}} + \nu\Delta\varepsilon_{\mathrm{y}} - \Lambda(S_{\mathrm{xx}} + \nu S_{\mathrm{yy}})] \\
\Delta\sigma_{\mathrm{y}} &= \frac{E}{(1-\nu^2)}[\Delta\varepsilon_{\mathrm{y}} + \nu\Delta\varepsilon_{\mathrm{x}} - \Lambda(S_{\mathrm{yy}} + \nu S_{\mathrm{xx}})] \\
\Delta\tau_{\mathrm{xy}} &= G(\Delta\gamma_{\mathrm{xy}} - \Lambda S_{\mathrm{xy}})
\end{aligned} \tag{18.7}$$

where S_{xx}, S_{yy}, S_{xy} are defined as

$$S_{\mathrm{xx}} = \frac{TC}{3}(k_1 + 2k_{11}\sigma_{\mathrm{x}} - k_{12}\sigma_{\mathrm{y}})$$
$$S_{\mathrm{yy}} = \frac{TC}{3}(k_2 + 2k_{22}\sigma_{\mathrm{y}} - k_{12}\sigma_{\mathrm{x}}) \tag{18.8}$$
$$S_{\mathrm{xy}} = 2TCk_{33}\tau_{\mathrm{xy}}$$

T and C denote the values of yield (failure) stress in tension and compression, respectively, determined for the characteristic of reference (see [18.10]).

For a material isotropic in the elastic range with the elastic-perfectly plastic characteristics the parameter Λ (which is a scalar, positively defined) is [18.10]

$$\Lambda = \frac{(S_{\mathrm{xx}} + \nu S_{\mathrm{yy}})\Delta\varepsilon_{\mathrm{x}} + (S_{\mathrm{yy}} + \nu S_{\mathrm{xx}})\Delta\varepsilon_{\mathrm{y}} + G^* S_{\mathrm{xy}}\Delta\gamma_{\mathrm{xy}}}{S_{\mathrm{xx}}^2 + 2\nu S_{\mathrm{yy}}S_{\mathrm{xx}} + S_{\mathrm{yy}}^2 + G^* S_{\mathrm{xy}}^2} \tag{18.9}$$

where: $G^* = G\left(1-\nu^2\right)/E$.

Rayleigh-Ritz variational method involving plasticity is applied to the problem. It was proved by Graves-Smith [18.8] that it is possible to apply the variational method to the plates undergoing finite deflections.

The potential energy in any point of a plate is a sum of elastic and plastic components. The plastic strain energy existing prior to the current strain increment bears no direct relation to the current state of stresses. For the purposes of minimisation this energy may arbitrarily be put to zero and only further changes of the strain energy have been taken into account.

$$\Delta W = \int_V \left[\left(\sigma_x + \frac{1}{2}\Delta\sigma_x \right)\Delta\varepsilon_x + \left(\sigma_y + \frac{1}{2}\Delta\sigma_y \right)\Delta\varepsilon_y + \left(\tau_{xy} + \frac{1}{2}\Delta\tau_{xy} \right)\Delta\gamma_{xy} \right] dxdydz \tag{18.10}$$

where: V - is a volume of the plate, $\sigma_x, \sigma_y, \tau_{xy}$ denote the stresses before the loading increment is applied and $\Delta\sigma_x, \Delta\sigma_y, \Delta\tau_{xy}$, $\Delta\varepsilon_x, \Delta\varepsilon_y, \Delta\gamma_{xy}$ denote the stress and strain increments produced by the increment of shortening ΔU_{c}.

In the elasto-plastic range the current state of stresses depends on the path of loading, so the solution of the problem can only be reached numerically. Therefore the numerical solution starts from the evaluation of the energy increment (10). In order to accomplish this, every layer is divided equally into $i \times j \times k$ appropriate cubicoids. The energy values calculated in each of cubicoids are summed for a whole structure.

Next, the numerical minimisation of the energy functional is performed versus independent parameter f of displacement functions. The average stress corresponding directly to the load applied to a considered structure is obtained numerically.

In each step of calculations active, passive and neutral processes and also the reduction of stress to the yield surface are taken into account.

18.3.2. Finite element method

The FE analysis of buckling, post-buckling and ultimate load of thin-walled members is usually solved in two steps:

- linear stability analysis (eigenvalue problem), which gives buckling loads (bifurcation points) and buckling modes (Fig. 18.3a [18.11]),
- non-linear stability analysis that allows to follow the behaviour of the structure in the post-buckling range and to find out the load carrying capacity.

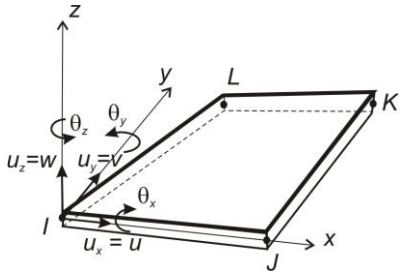

Fig. 18.2. Four-node shell element

Results of a linear buckling analysis (buckling loads and buckling modes) are used in the second step - non-linear analysis. The FE discrete model with the perturbation (geometric imperfections of the same shape as buckling modes determined in the first step) is applied. The analysis is carried out in order to determine the post-buckling path, the ultimate load and post-failure path. The imperfection amplitude is usually taken as 1/10 to 1/20 of the plate thickness. The FE model is built from shell elements. The simplest, typical shell element is shown in Fig. 18.2. It is a four-node element with six degrees of freedom at each node.

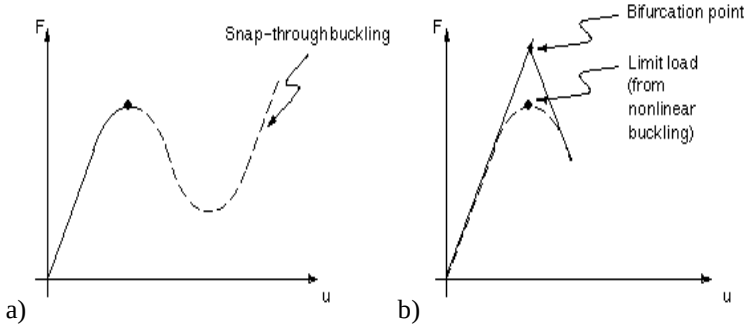

Fig. 18.3. Relations between forces and displacements in nonlinear and linear stability analysis using FEM [18.11]

In the present analysis the FE model was built of eight-node multi-layered shell elements of six degrees of freedom at each node (Fig. 18.4). This element allows to account for up to 100 layers of different thickness and material properties. In order to ensure the compatibility of boundary conditions considered in both methods the coupled degrees of freedom were assumed on the plate edges. It means that the distribution of applied compressive forces has to correspond to the uniform shortening of loaded edges and in the same time the unloaded edges should to remain straight and free of stresses. To describe a material stress - strain relationship the bilinear characteristic with plastic hardening [18.24, 18.25] was involved (Bilinear Kinematic Hardening option was used in ANSYS software).

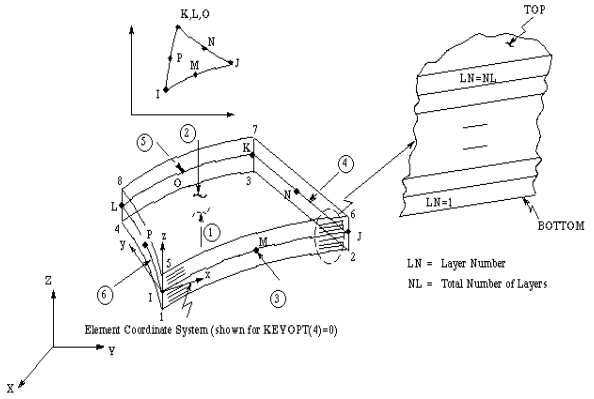

Fig. 18.4. Multi-layered shell element [18.24]

It should be added that in the post-buckling range the calculations were conducted using iteration scheme, the "arc-length" method, in order to avoid

bifurcation points and track unloading. The applied iteration method is represented schematically in Fig. 18.5 [18.24].

The numerical calculations were conducted using FE commercial code ANSYS. The value of the imperfection amplitude was equal to 1/20 of the thickness of an analysed structure.

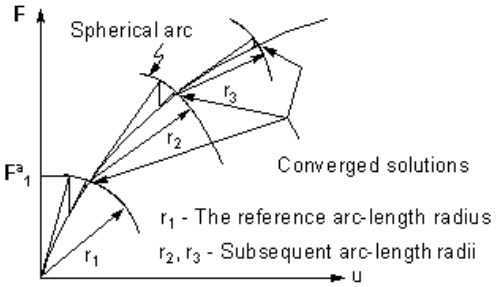

Fig. 18.5. Arc-length iteration method [18.24]

18.3.3. Plastic mechanism analysis

The kinematical method associated with the plastic mechanism approach (yield-line theory - YLT), has been used successfully to the analysis of ultimate load and post-failure behaviour of thin-walled structures since 60-ties of the 20th century [18.19]. This approach is attractive from some points of view, for it leads to relatively simple analytical or analytical-numerical solutions and provides not only with the upper-bound estimation of the ultimate load but with a knowledge about a rapidity of the failure process as well. The combination of the non-linear, post-buckling analysis with the analysis of the plastic mechanism allows one to establish a failure parameter approximately, i.e. to estimate the *upper bound* load-carrying capacity of the structure. Failure process in thin-walled, multi-layered structures may be of different character The failure modes of sandwich structures, depending on different layers configurations, materials of layers, span, etc., include face sheet yielding at large deformations (mainly for metal faces), face wrinkling, core shear leading to crack or yielding, core indentation. In the case of face sheets made of composite materials, one can detect delamination of faces. Another mode of failure is debonding on the contact surface between face sheet and core. Thus, among all failure modes mentioned above, a failure due to yielding (both in face sheets and core) can also take place in certain cases.

The kinematical method, based on the principle of virtual velocities [18.13, 18.19, 18.15], has been applied to the problem of the load-carrying capacity

estimation of multi-layered plated structures in association with the rigid-plastic theory. Thus, the following additional assumptions are taken in the analysis:

- yield occurs in all layers simultaneously, so that the continuity of plastic strains takes place (it limits the analysis to certain "sets" of materials),
- layers lay-out is symmetrical with respect to the plate middle surface and yield stresses increase with the increase of the distance from the centre layer,
- yield zones are not only concentrated at yield lines, but also at plastic zones of tensile stresses (true or quasi-mechanisms are taken into account).

In the case of the multi-layered plate subject to compression, from the principle of virtual velocities we obtain the following variational relation

$$\delta W_{ext} = \delta W_b + \delta W_m \tag{18.11}$$

where δW_{ext} is the variation of work of external forces, δW_b is the variation of the energy of bending plastic deformation, δW_m - variation of the energy of membrane plastic deformation.

The fully plastic moment capacity [18.13, 18.15] at concentrated yield-lines has been evaluated for multi-layered walls of the global plastic mechanism, under assumptions mentioned above.

$$\tilde{\tilde{m}}_p = m^0_{p\beta} + \sum_{i=1}^{n} \left\{ t_i \sigma_{0i} \cdot [t_0 + \sum_{j=1}^{i-1} (2t_j) + t_i] \right\} \tag{18.12}$$

where $m^0_{p\beta}$ is a fully plastic moment at the centre layer (generally orthotropic) which is expressed as follows

$$m^0_{p\beta} = \frac{\sigma^k_{00} t_0^2}{4} \qquad k = 1,2 \tag{18.13}$$

for yield-line parallel to principal directions of orthotropy with corresponding yield stresses σ^k_{00},

$$m^0_{p\beta} = \frac{\sigma_{\gamma 00} t_0^2}{4} \tag{18.14}$$

for yield-line inclined at angle γ to principal directions of orthotropy whereas $\sigma_{\gamma 00}$ is the yield stress for the direction γ that can be evaluated according to Hill

yield criterion [18.16]. The variation of the energy of bending plastic deformation dissipated at a yield-line amounts

$$\delta W_b = \sum_k l_k \overline{\overline{\underset{\sim}{m}}}_p \delta\beta_k \tag{18.15}$$

where l_k is a length of the yield-line and β_k is an angle of relative rotation of two walls of the global plastic hinge along that line.

In the case of three-layered wall with orthotropic core and taking into account the strain hardening phenomenon in face sheets, the plastic moment takes the form

$$\overline{\overline{\underset{\sim}{m}}}_p = m^0_{p\beta} + \left(\sigma_{01} + \frac{\overline{\sigma}_1 - \sigma_{01}}{2} \right) \cdot t_1 (t_0 + t_1) \tag{18.16}$$

where $m^0_{p\beta}$ is a fully plastic moment at the center layer (core), generally orthotropic, t_1, t_0 are facings and core thickness, respectively, σ_{01} - yield stress of the facing material. The effective stress $\overline{\sigma}_1$ is evaluated under assumptions taken by Kotełko [18.13, 18.16]

$$\overline{\sigma}_1 = \sigma_{01} + E_t \cdot \frac{\beta}{2n} \le \sigma_{ult} \tag{18.17}$$

where E_t is a tangent modulus and σ_{ult} is an ultimate stress of the facing material, β is an angle of rotation as in [18.15] and n is a multiple of the wall thickness.

Variation of plastic strain energy dissipated at plastic zones of membrane stresses in i-th layer takes form

$$\delta W_{m,i} = (N_{xi} \delta\varepsilon_x^p + N_{yi} \delta\varepsilon_y^p) A_p \tag{18.18}$$

where: N_{xi}, N_{yi} are membrane forces per unit length, A_{p} is an area of membrane stresses plastic zones. Membrane forces N_{xi}, N_{yi} can be determined using the associated flow rule for Huber-Mises yield criterion.

The total plastic strain energy dissipated at plastic zones of membrane stresses through the whole plate thickness is expressed as

$$\delta W_m = \delta W_{m0} + 2 \sum_{i=1}^{n} \delta W_{mi} \tag{18.19}$$

where: δW_{m0} - plastic strain energy in center layer, δW_{mi} - plastic strain energy in i-th layer.

Taking into account (18.12) to (18.19) in (18.11), a relation of compressive external force P in terms of shortening parameter (represented graphically as a *failure curve*) is evaluated.

An evaluation of the failure structural path (referred to as failure curve) can be used subsequently to the upper bound estimation of the load-carrying capacity of the plate or plated structure, namely an ordinate of the inter-section point of the failure curve with the post-buckling path obtained from the solution discussed in paragraph 3.2 is referred to as an upper bound ultimate load of the plate.

18.4. Selected numerical results

In this paragraph selected results of comparative numerical analysis carried out using three methods mentioned above, namely: analytical-numerical method (ANM), Finite Element Method (FEM) and kinematical method (KM) are presented for three-layered plates made of different materials. Point 4.9.3. concerns a particular problem of the three-layered plate with honeycomb core, solved using equivalent single plate models.

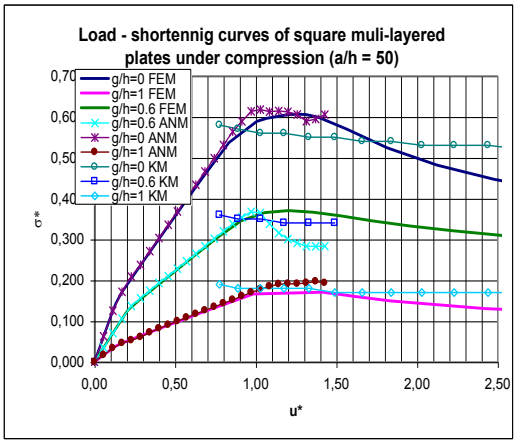

Faces - stainless steel
$E_m=2*10^5$ MPa; $\nu_m=0.3$
$\sigma_{Ym}=184$ MPa.

Core-aluminium
$E_c=7*10^4$ MPa $\nu_c=0.3$
$\sigma_{Yc}=123$ MPa.

Fig. 18.6. Load-shortening curves of square steel-aluminium-steel plate under compression [18.11]

18.4.1. Plates with metallic or fibrous composite core

Diagrams in Fig. 18.6 present the comparison of results obtained using different analytical methods and Finite Element Method for the plate with steel face sheets and aluminum core. Ratios g/h and a/h correspond to the notation in Fig. 18.1. The diagrams show the non-dimensional average stress normalized

with respect to face sheets yield stress $\sigma^* = \sigma_{av}/\sigma_{Ym}$ in terms of non-dimensional shortening coefficient $u^* = (u_c/a)/(\sigma_{Ym}/E_m)$ in the whole range of loading, including the failure phase. Diagrams present FE results (curves FEM), results of calculations of the load-capacity in the elasto-plastic range, based on the method, described in paragraph 18.3.1 [18.17] (curves ANM) and failure curves for the pitched-roof plastic mechanism [18.15], obtained using kinematical method, described in paragraph 18.3.3 (curves KM). In the kinematical approach the pitched-roof plastic mechanism model has been applied [18.15]. Three sets of diagrams are presented, corresponding to three different core thickness to total plate thickness ratio g/h.

Analogous diagrams in co-ordinate system $\sigma^* = \sigma_{cv}/\sigma_{Ym}$ in terms of $u^* = (u_c/a)/(\sigma_{Ym}/E_m)$ for the plate with composite core are shown in Fig. 18.7.

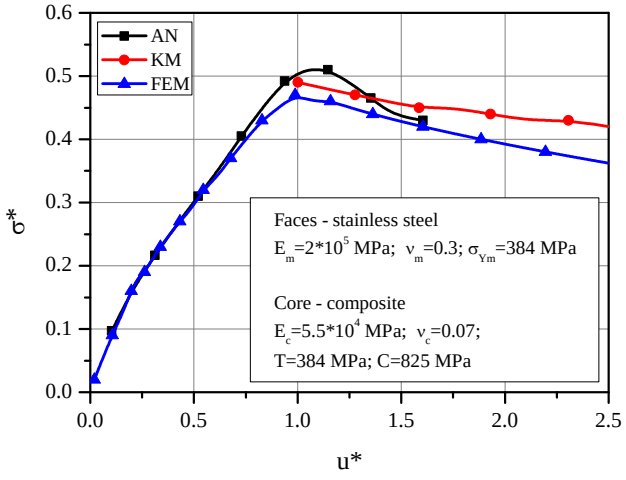

Fig. 18.7. Load-shortening curves of square metal-composite-metal plate under compression (a/h = 100) [18.11]

Analytical-numerical method (ANM) and FE simulations give very close results. The kinematical approach results, which are comparable with other results in the plastic range only, are also in relatively good agreement with two first methods.

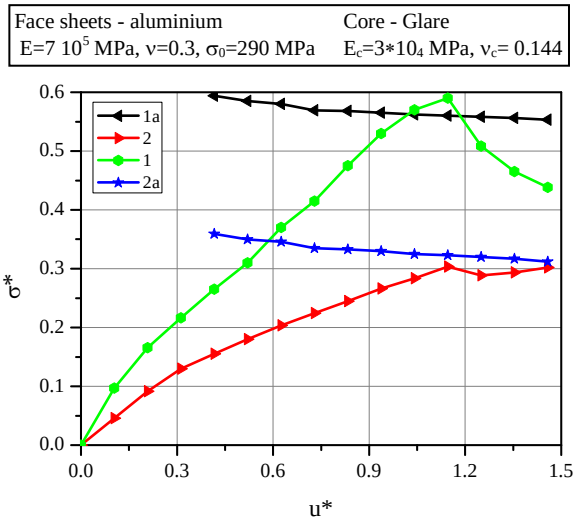

Fig. 18.8. Load-shortening diagrams of square metal-FML-metal plate under compression: a/h = 50; g/h = 0,4 (curves 1, 1a), g/h = 0,2 (curves 2, 2a); curves 1a,2a - kinematical method (KM), curves 1,2 - analytical-numerical method (ANM)

18.4.2. Plates with FML core

When a plate with GLARE core is subjected to the load, acting in its mid-plane, in the post-buckling state aluminium layers undergo yielding, while deformations of layers with glass fibers are still in the elastic range. Thus, structural behaviour of the plate with FML core differs substantially from the behaviour of the plate with homogeneous core [18.12]. In this paragraph very preliminary results of the analysis of structural behaviour of plates with FML core are presented. This analysis should be treated as a very far going approximation. The results concern also very particular parameters of plate layers and cannot be generalized. In Fig. 18.8 load-shortening diagrams in the coordinate system $\sigma^* = \sigma_{cv}/\sigma_{Ya}$ in terms of $u^* = (u_c/a)/(\sigma_{Ya}/E_a)$ are presented. Values of ultimate loads obtained using ANM and KM methods are very close (it should be underlined again, that equilibrium paths obtained from ANM and KM methods are comparable only in the plastic range). However, this agreement has to be confirmed in further analysis for wider range of plate dimensions, material parameters and layers configurations.

18.4.3. Plates with honeycomb core

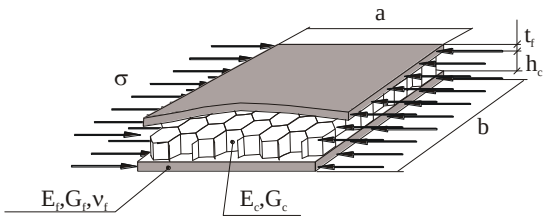

Fig. 18.9. Three-layered plate with honeycomb core

For inherently non-homogeneous structures like densely stiffened panel or three-layered plate with reinforced foam core, honeycomb core as well as corrugated metal sheet core a concept of structural orthotropy can be applied. It means, that one can calculate reduced orthotropic material parameters of the non-homogeneous structural member and subsequently consider the member as homogeneous but orthotropic one. Another words we can "smear" the non-homogeneity of the structure but take into account its orthotropy or generally, anisotropy. The problem of stability and load-capacity of sandwich structures with honeycomb core has been investigated by numerous researchers since 60-ties of the 20th century. Romanów [18.23] and Magnucki and Ostwald [18.17] carried out research in this domain. Romanów [18.11] has solved the problem of the sandwich plate with honeycomb core, using the energy method. Earlier Benson [18.20, 18.2] and Bert [18.3] worked on the same problem. The non-linear problem (of large deformations) of three-layered plate with orthotropic core have been solved by Alwan [18.1].

The problem of homogenisation of the honeycomb core strength characteristics was analyzed by Birger and Panovko [18.4] but has not been solved entirely so far. It seems that this problem as well as a homogenization of local failure phenomena could be solved using an averaging technique based on the asymptotic approach, however there has been very limited investigation into applications of this technique carried out.

Thus, simplified models that enable to avoid a complexity of the real sandwich structure are very much desirable and very attractive for designers under the circumstances discussed above. Two methods may be applied to replace the honeycomb sandwich panel by the equivalent single plate. There are namely: the equivalent rigidity method and the equivalent weight method (Vinson [18.26], Faulkner [18.5]), however limitations of these two approaches have not been entirely defined so far (Paik [18.21] and Kotełko and Mania [18.14]).

In the equivalent rigidity method the single plate equivalent thickness t_{eq} and equivalent Young modulus E_{eq} are defined such that the flexural rigidity of the equivalent plate given by the relation

$$D_{eq} = \frac{E_{eq} t_{eq}^3}{12(1-\nu_{eq}^2)} \tag{18.20}$$

(where $\nu_{eq} = \nu_f$) is equal to the flexural rigidity of the sandwich plate, calculated as (Paik [18.21])

$$D = \frac{E_f[(h_c + 2t_f)^3 - h_c^3}{12(1-\nu_f^2)} \tag{18.21}$$

Additionally, the shear stiffness of the equivalent plate is equal to the shear stiffness of facings. Thus, the parameters of the single plate are as follows [18.21]

$$\begin{aligned} t_{eq} &= \sqrt{3h_c^2 + 6h_c t_f + 4t_f^2} \\ E_{eq} &= \frac{2t_f}{t_{eq}} E_f \\ G_{eq} &= \frac{2t_f}{t_{eq}} G_f \end{aligned} \tag{18.22}$$

In the equivalent weight method the weight of the equivalent plate equals that of the actual sandwich plate so that the equivalent thickness amounts

$$t_{eq} = \frac{2t_f \rho_f + h_c \rho_{cav}}{\rho_f} \tag{18.23}$$

where ρ_f is a density of the facing material and ρ_{cav} is an average density of the core. The Young and shear moduli are assumed to be equal to those of the facing material ($E_{eq} = E_f$, $G_{eq} = G_f$).

A more realistic and accurate model of the sandwich panel is the three-layered plate with homogenized orthotropic core. In this study the homogenisation of the honeycomb core strength characteristics has been carried out using relations derived by Birger and Panovko [18.4]. Reduced elastic parameters of the core are determined assuming relative displacements of facings of the honeycomb sandwich panel to be equal to the corresponding displacements of three-layered plate with homogeneous orthotropic core. For example, in order to determine a shear modulus G_{xz} one has to calculate (using a certain method) relative displacements of facings in their mid-surfaces subject to loads applied in

these surfaces that cause distorsional (shear) relative displacements. The latter have to be compared with corresponding displacements in three-layered plate with homogeneous core. In an analogical way one can determine linear elastic moduli and Poisson ratios analyzing loads causing tension in the plate mid-surface or the normal direction.

Reduced elastic parameters used subsequently in FE analysis have been determined from following relations by Birger and Panovko [18.4]:

– shear moduli

$$G_{yz} = 0.576 G_c \frac{t_0}{r}; \quad G_{xz} = G_c \frac{t_0}{r} \xi \tag{18.24}$$

where t_0 is the thickness of the cell foil, $2r$ is the size of the hexagonal cell, ξ is a coefficient depending on structural parameters of the honeycomb core;

– linear module

$$E_x = E_y = 0 \qquad \text{for} \qquad \frac{h_c E_c t_0}{2 E_f t_f} < 0.25 \tag{18.25}$$

$$E_z = \frac{2 t_0 E_c}{1.3 r}$$

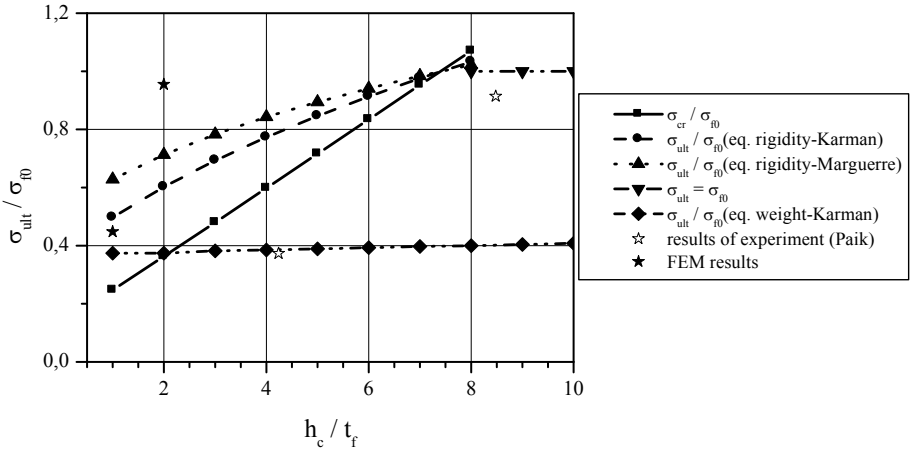

Fig. 18.10. Ultimate compressive stress predictions obtained from equivalent single plate models for square 500x500 mm sandwich plate with aluminium facings and honeycomb core made from aluminium foil t_f = 3 mm,
E_f = 71 070 MPa, σ_{f0} = 268 MPa, ρ_f = 2.7 g/cm^3, ρ_{cav} = 54.4.kg/m^3 [18.22]

The equivalent single plate models have been used by Kotełko and Mania [18.14] in order to determine buckling loads and load-bearing capacity of the

sandwich three-layered plate with the honeycomb core subject to compression (Fig. 18.9). The load-bearing capacity of equivalent single plates was determined using the effective width approach. The exemplary results for plates with equivalent rigidity and weight together with FE results obtained for three-layered plate with homogenized core are shown in Fig. 18.10.

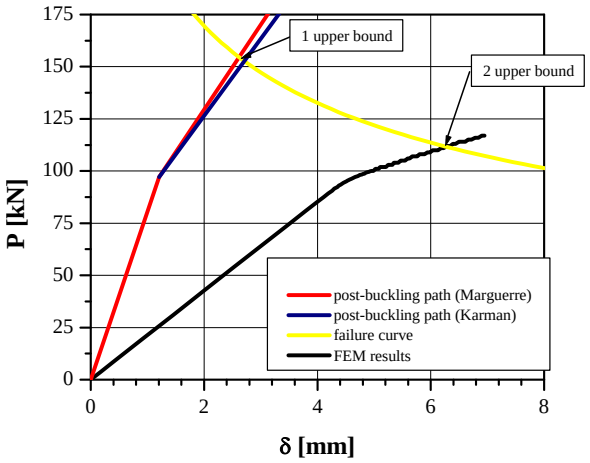

Fig. 18.11. Square plate 500x500 mm, h_C = 3, t_f = 1.5 mm, aluminium facings and honeycomb core made of aluminum foil (E_f = 71 070 MPa, σ_{f0} = 268 MPa), ρ_{cav} = 54 kg/m^3

The diagrams represent ultimate stress normalized with respect to facings material yield stress σ_{f0}, in terms of core to face thickness ratio. Ultimate stress has been calculated using von Karman [18.9] and Marguerre [18.18] relations for the effective width reduction factor. Diagrams obtained for both equivalent plate models are compared with FE results and experimental results [18.21]. Diagram of the normalized buckling stress, calculated using classical solution for the thin plate under uniform compression, concerns only the model of equivalent rigidity.

The FE analysis was performed in that case using reduced parameters of orthotropy, given by relations (18.11) and (18.12) in section 18.3.3. Hence, the material of facings was assumed isotropic and the core was modelled as homogenous orthotropic layer. The overall critical load and buckling mode of the plate was determined in the linear buckling analysis (eigen-value buckling). The non-linear buckling approach was employed for post-buckling response of the plate. The initial geometric imperfection for non-linear analysis was set as a first buckling mode shape with appropriate reduction coefficient.

Predictions of ultimate stresses obtained for the single plate model of equivalent weight underestimate an actual load-capacity of the sandwich panel

except the lowest values of h_c/t_f ratios, although experimental results even for $h_c/t_f = 4.35$ are very close to that prediction. However, it should be underlined here that both experimental ultimate loads indicated in the diagram concern the case of the failure initiated by the delamination while both theoretical models assume a perfect bonding between facings and the core. For higher values of h_c/t_f ratio greater than 3 the equivalent weight model is inadequate and gives ultimate load values more than two times lower than those obtained from equivalent rigidity model.

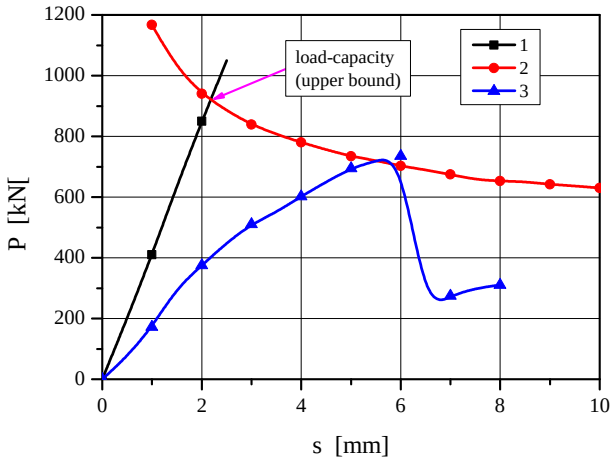

Fig. 18.12. Load-shortening diagram of square 500x500 mm sandwich plate with aluminium facings and honeycomb core made from aluminium foil t_f = 3 mm, h_c = 25.4 mm, E_f = 71 070 MPa, σ_{f0} = 268 MPa, ρ_f = 2.7 g/cm^3, ρ_{cav} = 54.4.kg/m^3

Structural behaviour of the sandwich plate in the entire range of loading (up to and beyond an ultimate load) has been examined using the effective width approach (for post-buckling state) and the kinematical approach (for the failure state). Pre-buckling paths were obtained taking into account compressive stiffness of facings only while compressive stiffness of the core was neglected. The single plate model of equivalent rigidity was applied as a more realistic one.

Post-buckling paths were calculated using the effective width approach with two different reduction factors, by von Karman [18.9] and Marguerre [18.18], respectively.

An exemplary diagram of the plate structural behaviour is shown in Fig. 18.11. Continuous straight line (1) represents the pre-buckling path, the failure curve (2) is obtained from the solution described in the previous

paragraph (kinematical approach). The ordinate of the intersection point indicated in the diagram represents the upper-bound estimation of the load-capacity of the sandwich plate. Theoretical pre-buckling and post-failure paths together with the failure curve form an approximate structural behaviour characteristics of the sandwich plate.

The discrepancy of results obtained for the single plate of equivalent rigidity and those obtained from FE calculations for the three-layered plate with homogenized orthotropic core is significant. However, the discrepancy concerns the stiffness of both equivalent plate and the three-layered plate with homogenized core. On the contrary, it is worthy to notice that buckling loads (folding points in both diagrams) are nearly the same for both cases. The discrepancy in magnitudes of upper bound estimations of ultimate loads obtained using the pre- and post-buckling path for the single plate of equivalent rigidity and the failure curve (from kinematical approach) and using FE results and the same failure curve amounts about 36%. More safe seems to be the second estimation: compilation of the failure curve and the post-buckling path obtained from FE analysis.

In this study the same approach has been used in order to analyse the load-capacity and failure of the simplified, approximate model of the sandwich panel, i.e. the model of two-layered plate consisting of facings of the real sandwich plate, the distance of which is maintained constant and equals the core thickness. Thus, the load-carrying capacity of the core is entirely neglected. The model applied is in fact a very "rough" approximation of real phenomena occurring in sandwich panels. However it enables to determine effectively a load-capacity of the sandwich panel in relatively simple analytical-numerical procedure.

Comparison of theoretical and experimental results obtained from the calculations based on this simplified model are shown in Fig. 18.12. Continuous straight line (1) represents the pre-buckling path, the failure curve (2) is obtained from the solution described in paragraph 18.3 (kinematical approach). The ordinate of the intersection point indicated in the diagram represents the upper-bound estimation of the load-capacity of the sandwich plate. Theoretical pre-buckling and post-failure paths form an approximate structural behaviour characteristics of the sandwich plate that is compared with experimental results obtained by Paik [18.21] - curve (3). The agreement of theoretical and experimental values of ultimate loads is reasonably good, although many factors influencing the sandwich panel structural behaviour were not taken into account in this approximate theoretical analysis.

18.5. Final remarks

The above chapter presents some selected results of the structural behaviour analysis of three-layered plates made of widely treated composite materials. It contains also the review of analytical-numerical methods, which can be applied in this analysis and are competitive with Finite Element simulations. However, the authors are aware of many simplifications assumed in those analytical-numerical methods. First of all, yielding is assumed as an only mode of failure, while in real plated structures made of composite materials one has to do with some other complex modes of failure, like face wrinkling, core shear leading to crack, core indentation, debonding on the contact surface between face sheet and core, etc. Thus, further research should be continued to include into the analytical-numerical models some of these phenomena. Also extension of those models into multi-layered plates built of orthotropic layers of different configuration is an open question.

18.6. References

18.1 Alwan A.M., Large deflection of sandwich plates with orthotropic cores, AIAA J. 2,10, 1964.

18.2 Benson A.S., Mayers J., General instability and face wrinkling of sandwich plates. Unified theory and applications, AIAA J., 5, 4, 1967.

18.3 Bert C.W., Cho K.N., Uniaxial compressive and shear buckling in orthotropic sandwich plates by improved theory, AIAA/ASME/ASCE/AHS, 27th Struct., Dyn. and Mat. Conf.,San Antonio, Tex., 1986.

18.4 Birger A.A., Panovko A.B., Strength, Stability, Vibrations. (in Russian), Masinostrojenie, Moskva 1968.

18.5 Faulkner D., A review of effective plating for use in the analysis of stiffened plating in bending and compression, J. Ship Res., 19, 1, 1975, pp. 1-17.

18.6 Grądzki R., Kowal-Michalska K., Stability and ultimate load of multi-layered plates - a parametric study, Engineering Trans., 51, 4, 2003, pp. 445-459.

18.7 Grądzki R., Kowal-Michalska K., Stability and ultimate load of multi-layered plates of constant mass, Proceedings of Fourth Intern. Conf. CIMS'2004, edited by: M.Pignataro, J.Rondal, V.Gioncu, Timisoara 2006.

18.8 Graves-Smith T.R., A variational method for large deflection elasto-plastic theory and its application to arbitrary flat plates, in Structure, Solid Mechanics and Engineering Design, Te'eni, M. ED., Wiley-Interscience, 1971, pp. 1249-1255.

18.9 Kármán T., Sechler E., Donnell L.H., The strength of thin plates in compression, Trans. ASME, 54, 1932, pp. 53-57.

18.10 Kołakowski Z, Kowal-Michalska K. (eds.), Selected problems of instabilities in composite structures. Series of Monographs. Technical University of Łódź 1999.

18.11 Kotełko M., Kowal-Michalska K., et al., Estimation of load carrying capacity of multi-layered plated structures, Thin-Walled Structures, Vol. 46, No 7-9, 2008, pp. 1003-1010.
18.12 Kotełko M., Kowal-Michalska K., Oszacowanie nośności granicznej płyt typu FML przy zastosowaniu metod analityczno-numerycznych (in Polish: Load-carrying capacity estimation of FML plates), XI Konferencja „Nowe Kierunki Rozwoju Mechaniki", Sarbinowo 2015, pp. 51-52.
18.13 Kotełko M., Load-capacity estimation and collapse analysis of thin-walled beams and columns - recent advances. Special Issue - Cold formed steel structures: recent research advances in Central and Eastern Europe, ed. By D. Dubina, Thin-Walled Structures Vol. 42/2, Elsevier 2004, pp. 153-175.
18.14 Kotełko M., Mania R.J., Limitations of equivalent plate approach to the load-capacity estimation of honeycomb sandwich panels under compression, Proc. of Fourth Int. Conf. on Thin-Walled Struct., Thin-walled structures - advances in research, design and manufacturing technology, J. Loughlan (ed.), Inst. of Physics Publishing, Bristol and Philadelphia 2004, pp. 679-686.
18.15 Kotełko M., Nośność i mechanizmy zniszczenia konstrukcji cienkościennych (in Polish: Load-capacity and mechanisms of failure in thin-walled structures), WNT, Warszawa 2010, ISBN 9 78-83-204-3681-5.
18.16 Kotełko M., Ultimate load and post-failure behaviour of thin-walled orthotropic beams, Int. J. Applied Mechanics and Engineering, 2001, Vol. 6, No. 3, pp. 693-717.
18.17 Magnucki K., Ostwald M., Stability and optimization of three-layered structures. (in Polish), Poznań-Zielona Góra 2001.
18.18 Marguerre K., Die mittragende Breite des gedruckten Platten-Streifens, Luftfahrtforschung (in German: Effective width of plate strip under compression), 14, 3, 1937.
18.19 Murray N.W., Introduction to the theory of thin-walled structures, Clarendon Press, Oxford 1986.
18.20 Okuto K., at al., The analysis and design of honeycomb welded structures, J. Light Met. Welding, Vol. 29, 8, 1991, pp. 361-368.
18.21 Paik J.K. at al., The strength characteristics of aluminium honeycomb sandwich panels, Thin-Walled Struct., Vol. 35, 1999, pp. 205-231.
18.22 Rhodes J., Effective widths in plate buckling; contribution to: Developments in thin-walled structures-1, edited by J. Rhodes and A.C. Walker, Applied Science Publishers, London 1981.
18.23 Romanów F., Strength of multi-layered structures (in Polish), Wyd. WSI Zielona Góra 1995.
18.24 Structural Analysis Guide for ANSYS rev. 5.7, Ansys Inc., Houston, USA.
18.25 Theory References release 5.6, Ansys Inc., Houston, USA.
18.26 Vinson J.R., The behaviour of sandwich structures of isotropic and composite materials, Technomic Publ. Comp., 1999.